

# Supporting information for Protein Handshake on the Nanoscale: How Albumin and Hemoglobin Self-Assemble into Nanohybrid Fibers

Christian Helbing<sup>1</sup>, Tanja Deckert-Gaudig<sup>2</sup>, Izabela Firkowska-Boden<sup>1</sup>, Gang Wei<sup>3</sup>, Volker Deckert<sup>2,4</sup>, Klaus D. Jandt<sup>1,5,6\*</sup>

<sup>1</sup> Chair of Materials Science (CMS), Otto Schott Institute of Materials Research, Faculty of Physics and Astronomy, Friedrich Schiller University Jena, Löbdergraben 32, 07743 Jena, Germany

<sup>2</sup> Leibniz Institute of Photonic Technology IPHT, Albert-Einstein-Strasse 9, 07745 Jena, Germany

<sup>3</sup> Faculty of Production Engineering, University of Bremen, Am Fallturm 1, 28359 Bremen, Germany

<sup>4</sup> Institute for Physical Chemistry and Abbe Center of Photonics, Friedrich Schiller University, Helmholtzweg 4, 07743 Jena, Germany

<sup>5</sup> Jena Center for Soft Matter (JCSM), Friedrich-Schiller-University Jena, Humboldtstraße 10, 07743 Jena, Germany

<sup>6</sup> Jena School for Microbial Communication (JSMC), Friedrich Schiller University, Neugasse 23, 07743 Jena, Germany

## RESULTS AND DISCUSSION

### AFM Images

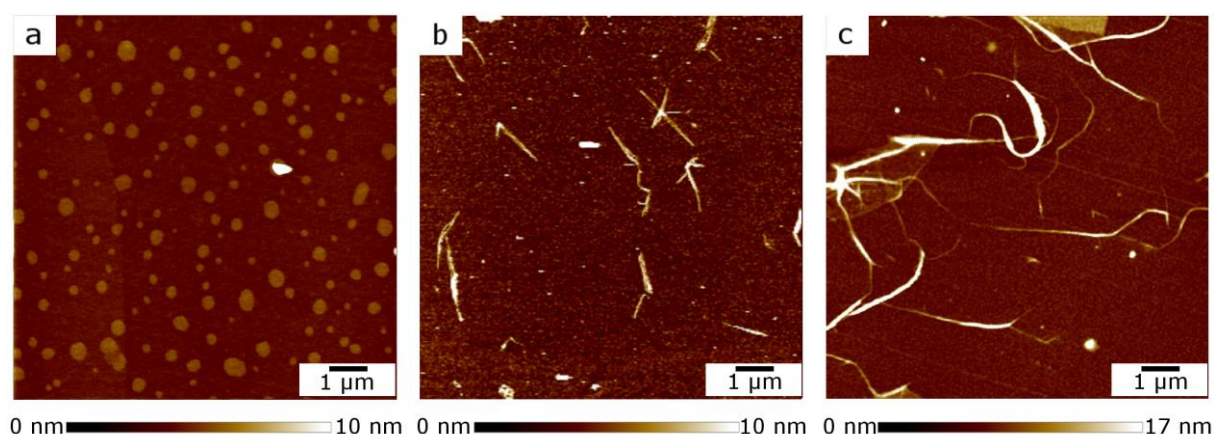


**Figure S1:** AFM height images of 100  $\mu\text{g/mL}$  HSA-HGB stored in 50 % ethanol at 65 °C and drop cast after different time periods: a) after 2 hours; b) and d) after 1 day; c) and e) after 7 days.

## TERS measurements of HSA-HGB and HSA fibers

**Table S1: Characteristic Raman bands of porphyrin and their corresponding assignments. Abbreviations:  $\nu$ , valence-vibration;  $\delta$ , deformation-vibration**

Raman shift [ $\text{cm}^{-1}$ ]	Local coordinate and assignment	Reference
660	$\delta(\text{pyrrol})_{\text{symmetric}}, \nu_7$	1
749	$\nu(\text{pyrrol breathing}), \nu_{15}$	1, 2
1128	$\nu(\text{C}_\alpha\text{N}), \nu_{22}$	1, 2
1312	$\nu(\text{C}_\alpha\text{C}_\beta), \nu_{21}$	1, 2
1355	$\text{Fe}^{2+}, \nu(\text{pyrrol half-ring})_{\text{symmetric}}, \nu_4$	2, 3
1378	$\text{Fe}^{3+}, \nu(\text{pyrrol half-ring})_{\text{symmetric}}, \nu_4$	2, 3
1545	$\nu(\text{C}_\beta\text{C}_\beta), \nu_{11}$	1

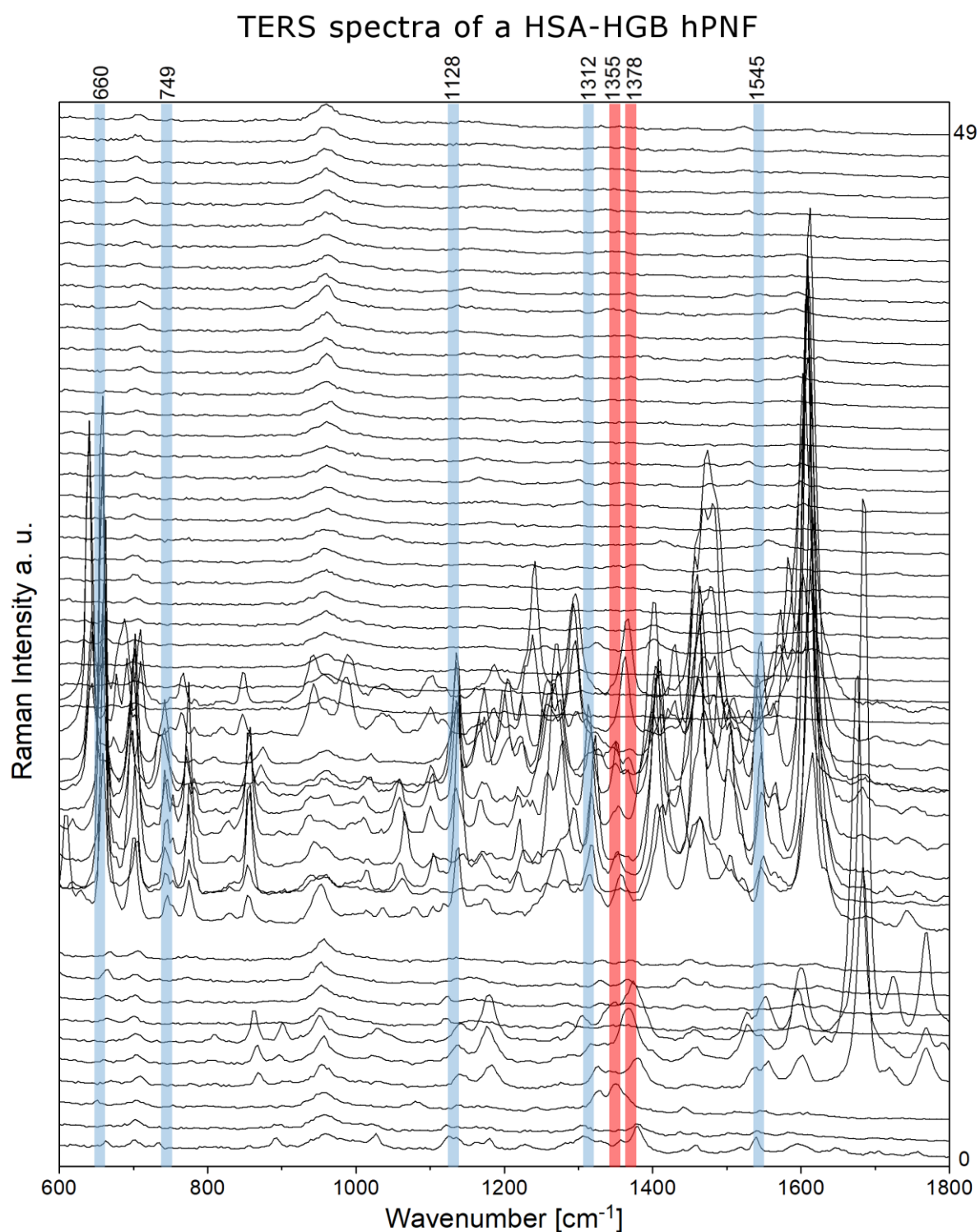


**Figure S2 | TERS characterization of HSA-HGB hPNFs:** TERS spectra collected along the marked line of the HSA-HGB hPNF in Fig. 2 from position 0 to 49 (step distance: 2.5 nm).  $\lambda = 532$  nm,  $P = 360$   $\mu\text{W}$ ,  $t_{\text{acq}} = 1$  s. In the shown spectra, corresponding marker bands for the porphyrin moiety (660  $\text{cm}^{-1}$ , 749  $\text{cm}^{-1}$ , 1128  $\text{cm}^{-1}$ , 1312  $\text{cm}^{-1}$ , 1545  $\text{cm}^{-1}$ ) are marked blue and for  $\text{Fe}^{2+}$  (1355  $\text{cm}^{-1}$ ) and  $\text{Fe}^{3+}$  (1378  $\text{cm}^{-1}$ ) are marked red. The bands between 1710 and 1745  $\text{cm}^{-1}$  are untypical for proteins and can be tentatively assigned to ester groups. The

appearance of those bands presumably originates from unexpected side reactions between the ethanol (solvent) and the carboxyl groups of the proteins. Since the laser power was two times lower compared to the laser power used for pure HSA-fibers, in spectra 24 - 49 signals are barely or not visible due to the absence of the photo-enhancing heme group.

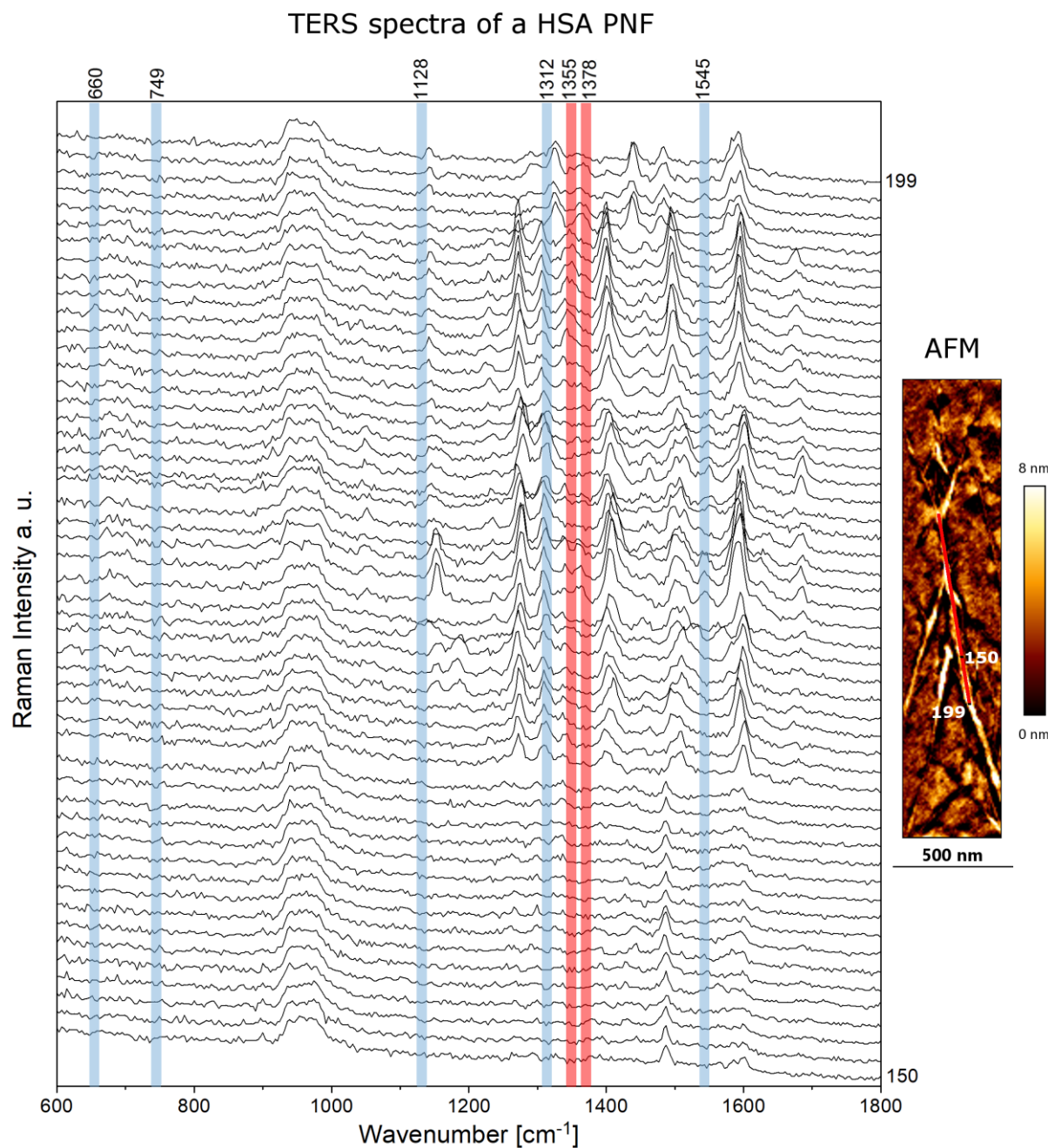


**Figure S3 | TERS characterization of HSA PNFs:** TERS spectra collected along the marked red line in the AFM height image of an HSA PNF from position 150 to 199 (step distance: 3.5 nm).  $\lambda = 532$  nm,  $P = 720$   $\mu$ W,  $t_{acq} = 1$  s. In the shown spectra, corresponding marker bands for the porphyrin moiety (660  $\text{cm}^{-1}$ , 749  $\text{cm}^{-1}$ , 1128  $\text{cm}^{-1}$ , 1312  $\text{cm}^{-1}$ , 1545  $\text{cm}^{-1}$ ) are marked blue and for  $\text{Fe}^{2+}$  (1355  $\text{cm}^{-1}$ ) and  $\text{Fe}^{3+}$  (1378  $\text{cm}^{-1}$ ) are marked red. (HSA PNFs

were prepared as described by Juárez *et al.*<sup>4)</sup> The absence of such modes indicates the difference between HGB and HSA.

### CD-Spectroscopy of HSA-HGB and Secondary Structure of HSA and HGB

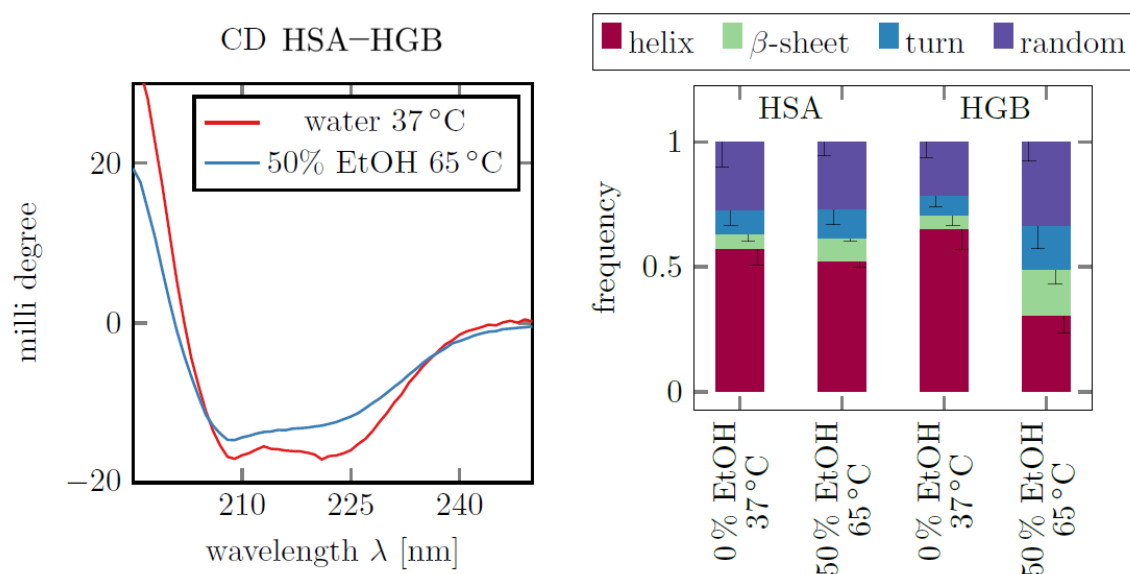


**Figure S4** | CD – spectroscopy of HSA-HGB mixtures and pure HSA and HGB: CD – spectroscopy of HSA-HGB mixtures in water at 37 °C (red) and in 50 % ethanol at 65 °C (blue). Secondary structure content of serum albumin and hemoglobin in water at 37 °C and in 50 % ethanol at 65 °C measured with CD.

To determine the secondary structure in the HSA-HGB PNF we performed CD-measurements. Figure S4 shows the resulting spectra for HSA-HGB in water at 37 °C and in 50 % ethanol at 65 °C. The differences in the signal correspond to a change in the secondary structure. The determination of the exact secondary structure amounts was not possible in a mixed protein solution. However, the minima at 208 and 221 nm indicate that proteins in the solution (water at 37 °C) consist mainly of helical structures. An increase of the temperature to 65 °C and addition of ethanol to a ratio of 50 vol% lead to a decrease of helical structures, corresponding to the disappearance of the minimum at 221 nm and the shift of the other minima from 208 nm to lower wavelengths (Fig. S4). Further, this shows that the content of  $\beta$ -sheet and loop-structures is increasing. These assumptions were verified by CD-measurements of the single proteins. Therefore, we investigated the influence of 50 % ethanol at 65 °C, the PNF formation conditions, compared to water 37 °C, (native conditions) on the secondary structure of the

single proteins. Their secondary structures under the selected conditions are shown in Fig. S4. In 50 % ethanol at 65 °C, HSA showed a minor change in the content of helical structures from 57 % (native) to 52 %. In addition, the amount of  $\beta$ -sheet structures slightly changed from 6 % (native) to 9 % (50 % ethanol 65 °C). In contrast, HGB showed a larger increase in  $\beta$ -sheet structures, compared to HSA, from 5 % (native) to 19 % (50 % ethanol 65 °C). Furthermore, the  $\alpha$ -helical structure content decreased from 65 % (native) to 30 % (50 % ethanol 65 °C). So, both proteins consist predominantly of helical structures under native conditions, which is in good agreement with the CD results for the HSA-HGB mixture. However, the single proteins showed a decrease in helical structures and an increase of  $\beta$ -sheets and turns under PNF formation condition, which contributes the observation from the HSA-HGB mixture spectra.

### **Force spectroscopy**

We performed AFM force spectroscopy measurements to determine the influence of HGB on the mechanical integrity of the hPNFs. Two representative force-distance curves are shown for HSA-HGB hPNFs and HSA PNFs in Fig. S5. It is conspicuous that both PNF types behave differently even though protein concentration, self-assembly time and conditions as well as measuring conditions were similar. The measured forces can be explained in two different ways: (1) as pull-off force, which is needed to retract the PNF-modified tip from the modified Si-surface or (2) as rupture force, which is needed to tear the PNF. The measured pull-off or rupture-forces of HSA PNFs were four times higher ( $158.4 \pm 46.1$  nN) than for HSA-HGB hPNFs ( $38.97 \pm 9.67$  nN). Furthermore, it is visible that the retraction length, which is needed to pull the (h)PNFs from the modified Si-surface or to tear the (h)PNF, is also higher for HSA PNFs (larger than 13.5  $\mu$ m) compared to the hPNFs (6.9  $\mu$ m). As a result, we can sum up that the incorporation of HGB into the hPNFs leads to a decreased mechanical integrity.



## AFM Force Spectroscopy

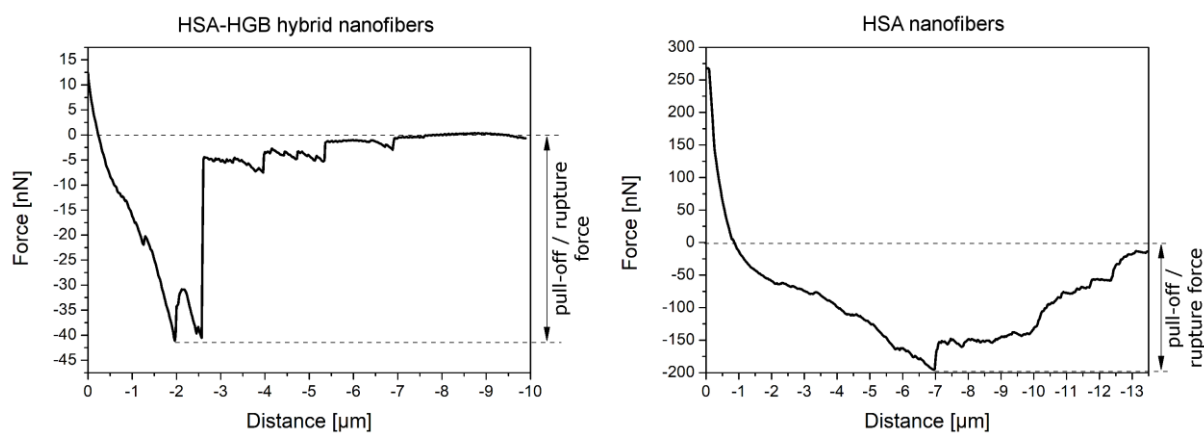


**Figure S5 | Force spectroscopy of HSA-HGB hPNFs and HSA-PNFs:** AFM force-distance curves for the retraction of modified with HSA-HGB (left) and HSA (right) PNFs from the modified Si-substrate. The pull-off / rupture forces are marked in both graphs.

## Amino Acid Sequences of HSA and HGB

Figure S6 shows the amino acid sequences of HSA and the alpha and beta domains of HGB, HGB consists of two alpha and two beta domains. The uniprot alignment tool<sup>i</sup> was used to compare both proteins. Regions which are identical are marked with an “\*”, very similar regions marked with an “:” and only similar regions are marked with an “.”. The comparison of HSA and the HGB alpha domains shows that both proteins have similar regions (marked with a red rectangle Fig. S6), especially in the middle part at the amino acids 31-119 of alpha HGB and 241-325 of HSA. Similar regions were further found for the sequences 7-91 of beta HGB and 25-114 of HSA. It is possible that these regions are responsible for the interactions between both proteins during the fiber formation. Furthermore, Fig. S6 shows that both proteins consist of amino acids with hydrophobic properties based on their residues (amino acids marked purple in Fig. S6). So, we assume that hydrophobic interactions are the dominant interactions between both proteins. This assumption is strengthened by analysing the amount of hydrophobic, polar and charged amino acid residues in the single proteins, which are shown in Table S2. Both proteins, HSA and HGB, mainly consist of amino acids with hydrophobic

residues, 42 % and 54 %, respectively. The lower content of polar, 27% for HSA or HGB and charged amino acid residues, 31% for HSA and 19% for HGB, shows the negligible role of hydrogen bonds and electrostatic interactions on fiber formation.

**Table S2: amount of hydrophobic, polar and charged amino acid residues in HSA and HGB**

	<b>hydrophobic amino acids</b>	<b>polar amino acids</b>	<b>charged amino acids</b>
<b>HSA</b>	<b>42 %</b>	<b>27 %</b>	<b>31 %</b>
<b>HGB</b>	<b>54 %</b>	<b>27 %</b>	<b>19 %</b>



**Figure S6 | Amino acid sequences of HSA and HGB:** Comparison of HSA amino acid sequences with HGB alpha and beta domains. Thereby, the "\*" means complete agreement, ":" very similar; "." similar. Additionally, all similar amino acids are marked by a red rectangle. Hydrophobic amino acids are marked purple.

## REFERENCES

1. Drescher, D.; Buchner, T.; McNaughton, D.; Kneipp, J., SERS Reveals the Specific Interaction of Silver and Gold Nanoparticles with Hemoglobin and Red Blood Cell Components. *Phys. Chem. Chem. Phys.* **2013**, *15*, 5364-5373.
2. Rygula, A.; Majzner, K.; Marzec, K. M.; Kaczor, A.; Pilarczyk, M.; Baranska, M., Raman Spectroscopy of Proteins: A Review. *J. Raman Spectrosc.* **2013**, *44*, 1061-1076.
3. Wood, B. R.; Asghari-Khiavi, M.; Bailo, E.; McNaughton, D.; Deckert, V., Detection of Nano-Oxidation Sites on the Surface of Hemoglobin Crystals Using Tip-Enhanced Raman Scattering. *Nano Lett.* **2012**, *12*, 1555-1560.
4. Juarez, J.; Alatorre-Meda, M.; Cambon, A.; Topete, A.; Barbosa, S.; Taboada, P.; Mosquera, V., Hydration Effects on the Fibrillation Process of a Globular Protein: The Case of Human Serum Albumin. *Soft Matter* **2012**, *8*, 3608-3619.

---

<sup>i</sup> <http://www.uniprot.org/>